Adaptive Manufacturing Method for Double Diaphragm Forming of CYCOM® EP2750 Prepreg

Y. Jiang[1], S. El Euch[1], K. Dupuis[2], B. Gourichon[2], M. Mercado[1] and F. LeBel[1*]

[1] Centre technologique en aérospatiale, 5555 rue de l'ENA, Saint-Hubert, Quebec, Canada,
[2] Syensqo, 7140 rue Albert Einstein, Montreal, Quebec, Canada

* *François LeBel (francois.lebel@aerocta.ca)*

Keywords: *adaptive manufacturing; double diaphragm forming (DDF); fast-curing prepreg; prepreg aging*

1. Abstract

The rapid growth of Advanced Air Mobility industry is increasing demand for fast-curing composite systems and high-rate manufacturing processes. To address this, Syensqo has developed the CYCOM® EP2750 fast curing prepreg and the corresponding Double Diaphragm Forming (DDF) process. This work develops an adaptive DDF approach for EP2750 prepreg to maintain part quality throughout prepreg aging. 18 omega-shaped parts were manufactured from prepregs aged for 0 (fresh), 6, 12 and 20 days. Gap dwell duration and preheating conditions were adjusted using previously developed material models [1], based on viscosity and flow index at the onset of consolidation as processability indicators.

Part quality was evaluated through dimensional survey, ultrasonic inspection, and mechanical testing. Best-parameter parts from all aging stages achieved thicknesses within ±2.4% of the reference. Ultrasonic inspection showed minimal aging-related variation in the top flange region. Mechanical properties, including short-beam strength, unnotched tensile, open-hole tensile, and open-hole compressive strength, remained within acceptable ranges across all aging stages, with no significant aging-driven degradation. Overall, the results demonstrate that model-informed adaptive manufacturing method significantly extends the processability window of EP2750 prepregs while maintaining acceptable part quality and mechanical performance.

2. Background

Advanced Air Mobility (AAM), including drones and electric vertical take-off and landing (eVTOL) vehicles, is driving demand for high-rate composite manufacturing at competitive cost and aerospace quality. Out-of-autoclave (OoA) processes have drawn strong interest for reducing cycle time, cost, and energy consumption versus autoclave processing [2–3]. However, the inherent variability of prepregs and part manufacturing processes requires robust quality control to consistently achieve aerospace-level quality at high rate. Prepreg aging during storage and handling alters viscosity and flow behavior, increasing the risk of non-conforming parts when fixed process parameters are used. Adaptive manufacturing addresses this by tuning process parameters based on the actual material state. Recent studies show OoA reliability depends on precise material-state monitoring and rigorous process control [4–6]. Among OoA processes, DDF shows strong potential for aerospace [7]. Syensqo has developed the fast-curing aerospace-grade epoxy prepreg CYCOM® EP2750 and the DDF process as a coupled material-process solution for high-rate manufacturing of complex parts. In a previous study [1], the authors developed cure kinetics, viscosity, glass transition, and fiber bed compaction models for CYCOM® EP2750. Building on this, the present work proposes a model-informed adaptive DDF strategy that adjusts preheating conditions and gap dwell duration based on viscosity and flow index to preserve part quality up to 20 days of aging. This approach reduces material waste and helps identify the processability limit beyond which defect-free production cannot be guaranteed.

3. Materials and methods

3.1. Materials

CYCOM® EP2750 2x2 twill weave carbon-fiber/epoxy prepreg was used throughout this study. Rolls were stored at -18 °C and thawed at room temperature for 16-20 hours prior to cutting. Plies were cut using a Gerber DCS 2500 automated cutting table and grouped into laminate kits. A set of kits was returned immediately to the freezer as the 0-day reference. The remaining kits were aged at 21°C and 45% relative humidity for 6, 12, and 20 days. Plies were assembled into a laminate following a defined stacking sequence, adapted to the omega-shaped tooling geometry (Figure 1(b)), including a ramp section representative of a thickness transition (ply drop). The base laminate consisted of 16 plies arranged as $(45/0)_{4s}$, with additional local 0° doublers creating a transition from 24 to 16 plies (Figure 1(a)).

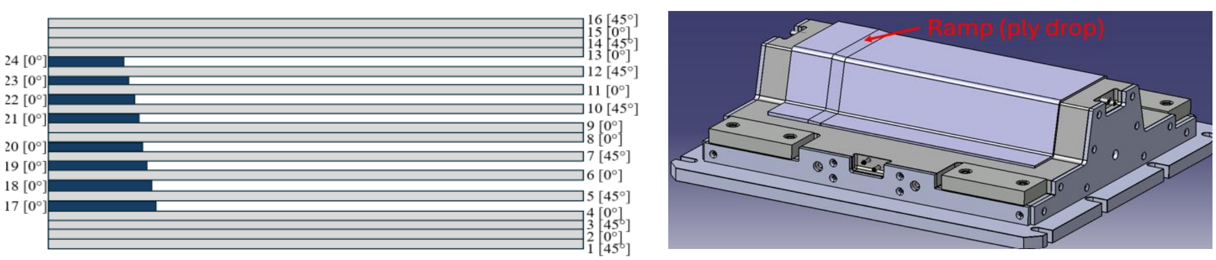

(a) (b)

Figure 1. (a) Schematic of the laminate stacking sequence (ply thickness and dimensions are not to scale) and (b) Lower half of the omega shaped tooling used for part manufacturing.

3.2. Double Diaphragm Forming (DDF) process

Each laminate kit was formed using a DDF setup consisting of a DDF frame, a self-developed infrared (IR) oven, and an omega-shaped tooling mounted on a 150-ton Wabash Press. The DDF process consists of three stages: preheating, gap dwell, and consolidation. The laminate enclosed between two flexible diaphragms is preheated in the IR oven to reduce resin viscosity and promote ply drapability, then transferred to the press for gap dwell, where a 2 mm gap is maintained between the tool surfaces to promote resin redistribution and inter-ply contact. Finally, the gap is closed, and tonnage is applied to consolidate the laminate. A nominal DDF cycle was established using fresh prepreg as the reference condition. For aged prepregs, preheating conditions and gap dwell duration were adjusted per Section 3.3, with all other parameters held constant.

3.3. Adaptive manufacturing strategy

As EP2750 prepreg ages, progressive resin advancement increases degree of cure $\alpha(t)$ and viscosity $\mu(\alpha, T)$, reducing flow capability and increasing the risk of porosity, thickness non-uniformity, and wrinkling. To compensate, preheating conditions and gap dwell duration were adjusted using viscosity and flow index [8] ($F.I. = \int_{t_o}^{t_f} \frac{1}{\mu(\alpha(t),T(t))} dt$ where T and t are temperature and time respectively) at consolidation onset as material state indicators, derived from the EP2750 material models [1].

A two-stage design of experiments (DOE) approach was employed. In DOE 1, preheating was fixed at 95 °C for 5 mins, while gap dwell duration was varied per aging group. Shorter duration results in lower viscosity and higher flow index at consolidation onset. In DOE 2, the optimized gap dwell duration was maintained, and preheating was modified to 120 °C for 2 mins, further lowering viscosity and increasing flow index, based on the material models. A total of 18 parts were manufactured. The process parameters are summarized in Table 1.

Table 1. DDF process parameters for all 18 manufactured parts, grouped by aging conditions.

Prepreg	**Part no.**	**DOE**	**Preheating**		**Gap dwell**		**Normalized Viscosity***	**Normalized Flow index***
			Temp (°C)	**Time (min)**	**Temp (°C)**	**Time (min)**		
0-day aged								
	P01	DOE 1	95	5	180	5	1.48	0.60
	P02	***Reference***	95	5	180	4	1.00	1.00
	P12	DOE 2	120	2	180	4	0.99	1.01
	P16	DOE 2	120	2	180	4	0.99	1.01
6-day aged								
	P03	DOE 1	95	5	180	2.5	1.43	0.63
	P04	DOE 1	95	5	180	4.5	3.96	0.18
	P05	DOE 1	95	5	180	3.5	2.27	0.35
	P13	DOE 2	120	2	180	3.5	1.96	0.42
	P18	DOE 2	120	2	180	2	1.10	0.25
12-day aged								
	P06	DOE 1	95	5	180	3.5	4.69	0.14
	P07	DOE 1	95	5	180	2.5	2.62	0.29
	P08	DOE 1	95	5	180	1.5	1.61	0.54
	P14	DOE 2	120	2	180	1.5	1.41	0.63
	P17	DOE 2	120	2	180	2	1.91	0.43
20-day aged								
	P09	DOE 1	95	5	180	2.5	6.89	0.09
	P10	DOE 1	95	5	180	1.5	3.65	0.20
	P11	DOE 1	95	5	180	1	3.01	0.25
	P15	DOE 2	120	2	180	1	2.56	0.30

*Viscosity and flow index values are normalized relative to the reference condition (P02), for which both values are set to 1. Viscosity and flow index correspond to onset of consolidation.

3.4. Inspection and characterization

Part quality was evaluated through thickness measurements, non-destructive ultrasonic inspection, and mechanical testing.

3.4.1 Dimensional survey

Part thicknesses were measured on all 18 parts using a thickness gauge at 20 discrete locations per part (Figure 2 (left)). In the 24-ply region, 5 measurements were taken across the cross-section: one on each foot flange, one on each vertical flange, and one on the top flange. In the 16-ply region, 15 measurements were taken.

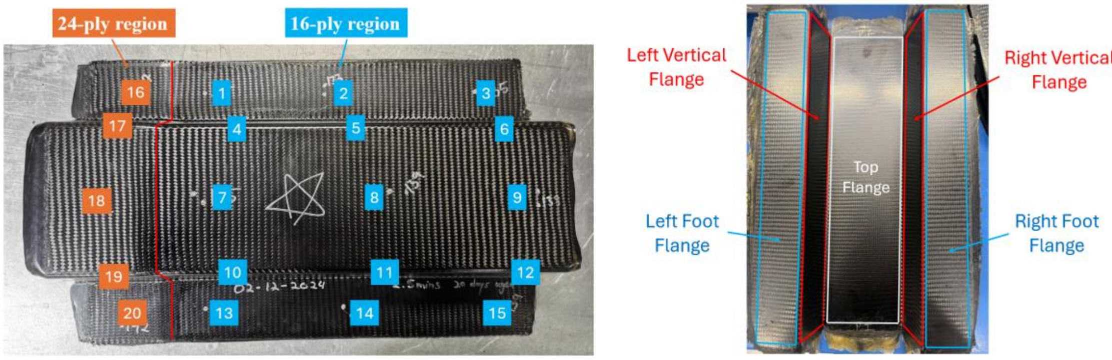

Figure 2. (left) Illustration of 20 thickness measurement locations and (right) Illustration of the different geometric zones of the manufactured part intended for inspections.

3.4.2 Ultrasonic inspection

Relative part quality was assessed on 14 of the 18 manufactured parts: P1-5, P7-13, P15 and P17, using non-destructive ultrasonic inspection based on longitudinal wave attenuation through the laminate thickness. The inspections were performed using an immersion phased-array pulse-echo technique with a linear probe (5 MHz, 64 elements) and a Topaz 32/128 PR ultrasonic system (Zetec), with data acquisition via UltraVision software.

Two regions were inspected: top flange (zone 1) and left vertical flange (zone 2), shown in Figure 2. All inspections were conducted in an immersion water tank, with a constant water path of 110 mm maintained between probe and specimen (Figure 3). Ultrasonic data was acquired over a 2D grid with 1 mm resolution, enabling the generation of 2D ultrasonic maps of the inspected regions.

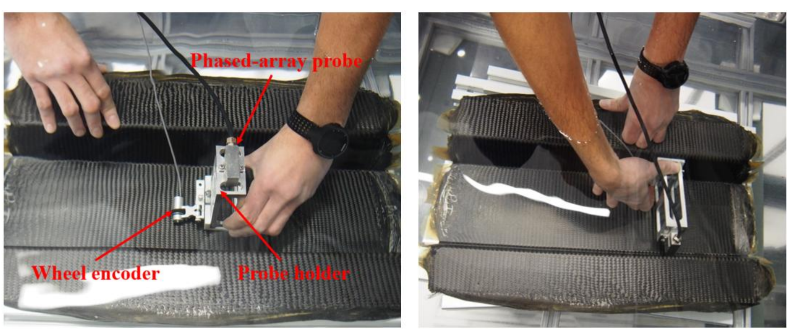

(a) (b)

Figure 3. Experimental setup used for ultrasonic inspection of the omega-shaped composite parts: (a) inspection of the top flange (Zone 1); (b) inspection of the left vertical flange (Zone 2).

Ultrasonic data was analyzed using a pulse-echo method based on the amplitude ratio between the front-wall and back-wall echoes. Assuming comparable laminate thickness across all parts, differences in amplitude ratio were attributed primarily to variations in porosity. Amplitude ratios are reported as absolute values, where higher values indicate higher relative porosity.

3.4.3 Mechanical testing

Prior to mechanical testing, all 18 parts were post-cured freestanding in an oven at 180 °C for 60 minutes. Mechanical tests were performed on 12 selected parts: P1-3, P5, P7-9, P11-13, P15 and P17, representing all four aging conditions and both DOE stages. Test specimens were extracted using abrasive waterjet cutting. Holes for open-hole tests were machined using a reamer.

Four mechanical test types were performed: short-beam strength (SBS), unnotched tensile strength (UNT), open-hole tensile strength (OHT), and open-hole compressive strength (OHC). Test parameters are summarized in Table 2. For all tensile and compressive tests, specimens were sourced from the 16-ply zone with a grip separation of 200 mm and tested at 2 mm/min. SBS specimens were sourced from the 24-ply zone and tested at 1 mm/min.

Table 2. Mechanical test parameters summary.

Test	Standard	Instrument	Specimen length (mm)	Specimen width (mm)	Hole diameter (mm)	Test speed (mm/min)
Short-beam strength (SBS)	ASTM D2344	Instron 5900R/5584	40	10	/	1
Unnotched tensile strength (UNT)	ASTM D5766	Instron 5985	300	36	/	2
Open-hole tensile (OHT)	ASTM D5766	Instron 5985	300	36	6	2
Open-hole compression (OHC)	ASTM D6484	Instron 5985	300	36	6	2

Six SBS specimens per part were extracted from the 24-ply zone, with one specimen from each foot flange, one specimen from each vertical flange, and two specimens from top flange. Tests were conducted with a loading nose diameter of 6.35 mm, support pin diameter of 3.17 mm, and support span of 18.00 mm. Two UNT specimens per part were extracted from the top flange of the 16-ply zone and tested following a modified configuration of ASTM D5766, in which no hole was drilled. This modification enables characterization of the tensile property of the laminate without the influence of stress concentrations introduced by an open hole. Two OHT specimens per part were extracted from the 16-ply zone, one from the foot flange and one from the vertical flange. Two OHC specimens per part were extracted from the 16-ply zone, one from the foot flange and one from the vertical flange.

4. Results and discussion

4.1. Dimensional survey

Thickness measurements were performed on all 18 parts at 20 locations per part: 15 points in the 16-ply region and 5 points in the 24-ply region. First, the average laminate thickness across all parts per aging stage was calculated to assess overall dimensional variations. Then, a focused comparison of the best-parameter parts from each aging stage against the reference (P02, 0-day, nominal recipe) was conducted to evaluate the effectiveness of the adaptive manufacturing strategy. Best-parameter parts are defined as parts with lowest viscosity and highest flow index at the onset of consolidation within each aging group: P12 (0-day), P03 (6-day), P08 (12-day), and P15 (20-day). The results are presented in Figure 4. For the best-parameter parts, 95% confidence intervals were computed using the Student's t-distribution (n = 15 for 16-ply, n = 5 for 24-ply).

Error bars are not shown for the group means, as the within-group spread results from intentional process parameter variation rather than uncontrolled scatter, and would therefore be misleading if presented as a measure of process repeatability.

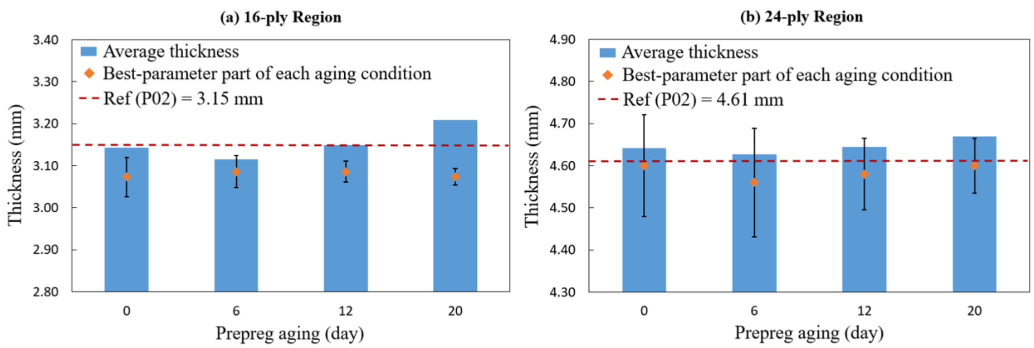

Figure 4. Part thickness by prepreg aging stages for the (a) 16-ply region and (b) 24-ply region.

At the group level, average thickness remained close to the reference across all aging conditions, ranging from 3.11 mm to 3.20 mm (16-ply) and 4.61 mm to 4.66 mm (24-ply), with no systematic trend across the out-life.

At the individual level, the four best-parameter parts achieved thicknesses close to reference within ±2.4% in the 16-ply region and ±1.3% in the 24-ply region, demonstrating effective dimensional quality throughout the 0 to 20 day out-life. In contrast, the two parts with the highest viscosities, P06 and P09, showed significantly larger thickness deviations from the reference, up to 9%, reaching 3.42 mm and 3.44 mm in the 16-ply region. This is consistent with reduced compaction associated with reduced material flowability at high viscosity. These observations further support the importance of maintaining sufficient material flow capability using adaptive manufacturing strategy during the DDF process.

4.2. Ultrasonic inspection

Relative part quality was assessed on 14 of the 18 manufactured parts using non-destructive ultrasonic inspection. The absolute value of the amplitude ratio was used as the porosity indicator, where a higher value indicates greater signal attenuation and higher relative porosity. Results are listed in Table 3, grouped by aging condition and sorted by ascending viscosity within each group, so that the within-group trend between material model indices and amplitude ratios is more visible.

As shown in Figure 5, in Zone 1, amplitude ratios show no statistically significant variation across aging stages. The absence of a monotonic trend suggests that the adapted parameters were effective at improving relative part quality in the top flange region. The high within-group variability reflects the deliberate within-group process parameter variation rather than uncontrolled scatter. Parts manufactured with intentionally poor parameters (e.g. P09, high viscosity, used to study the viscosity – relative part quality correlation) exhibit higher amplitude ratios as expected. Focusing on the best-parameter part from each aging group, amplitude ratios of P03 (6-day), P08 (12-day), and P15 (20-day) are all close to the best 0-day part P12. This confirms that when appropriate process parameters are applied, top flange quality is well maintained across the full out-of-freezer aging range.

As can be seen in Figure 5, Zone 2 amplitude ratios show a slight increasing trend with aging stage. However, the interpretation of this trend requires caution. Since the amplitude ratio was not normalized by part thickness, higher values could be partly caused by the increased path length in thicker parts rather than a genuine increase in porosity. The 12-day and 20-day parts exhibit slightly higher thickness than the 0-day and 6-day parts, which could contribute to the observed increase in amplitude ratio. However, all best-parameter parts from 0–20 day aging remain within a relatively narrow range. This suggests that the adapted parameters appear to keep Zone 2 within an acceptable and repeatable relative part quality up to 20 days of aging, with some uncertainty on the microstructure defect type involved that requires further investigation and validation through cross-sectional validation.

Table 3. Ultrasonic inspection results of the 14 assessed parts, grouped by aging condition and sorted by ascending viscosity within each group.

Prepreg	Part no.	Normalized Viscosity	Normalized Flow index	Zone 1 Amplitude ratio (dB)†	Zone 2 Amplitude ratio (dB)†
0-day aged					
	P12*	0.99	1.01	5.84	5.29
	P02 (ref)	1.00	1.00	5.85	5.39
	P01	1.48	0.60	6.72	5.47
6-day aged					
	P03*	1.43	0.63	5.46	5.35
	P13	1.96	0.42	6.44	5.35
	P05	2.27	0.35	5.68	5.57
	P04	3.96	0.18	6.00	5.54
12-day aged					
	P08*	1.61	0.54	5.42	5.71
	P17	1.91	0.43	5.70	5.83
	P07	2.62	0.29	5.83	5.76
20-day aged					
	P15*	2.56	0.30	5.56	5.97
	P11	3.01	0.25	5.61	6.07
	P10	3.65	0.20	6.02	6.09
	P09	6.89	0.09	7.38	6.49

* Best-parameter part (lowest viscosity and highest flow index) within each aging group.
† Amplitude ratios are reported as absolute values, where higher values indicate greater signal attenuation.

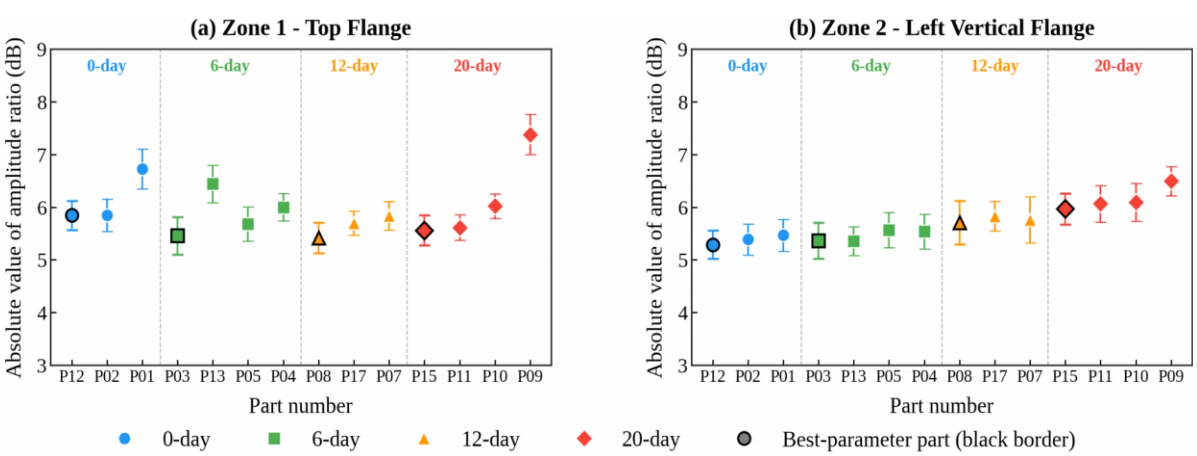

Figure 5. Absolute value of amplitude ratio of the 14 assessed parts grouped by aging stage: (a) Zone 1 - top flange and (b) Zone 2 - left vertical flange.

4.2.1 Correlation with material model indices

Figure 6 shows the amplitude ratio of each part as a function of normalized viscosity at consolidation onset for both zones. A strong positive correlation was found between normalized viscosity and Zone 2 amplitude ratio. Higher viscosity leads to greater amplitude ratio. In contrast, weak correlation was found for Zone 1. Within each aging group, the part with the lowest viscosity consistently achieved the lowest amplitude ratio in both zones (Table 3). As mentioned in section 4.1, these four best-parameter parts also produced thicknesses closest to the reference value. This result provides direct within-group validation that reducing viscosity and increasing flow index through adaptive preheating and gap dwell adjustment leads to measurably improved part quality and better dimensional conformance, independently of the aging stage itself.

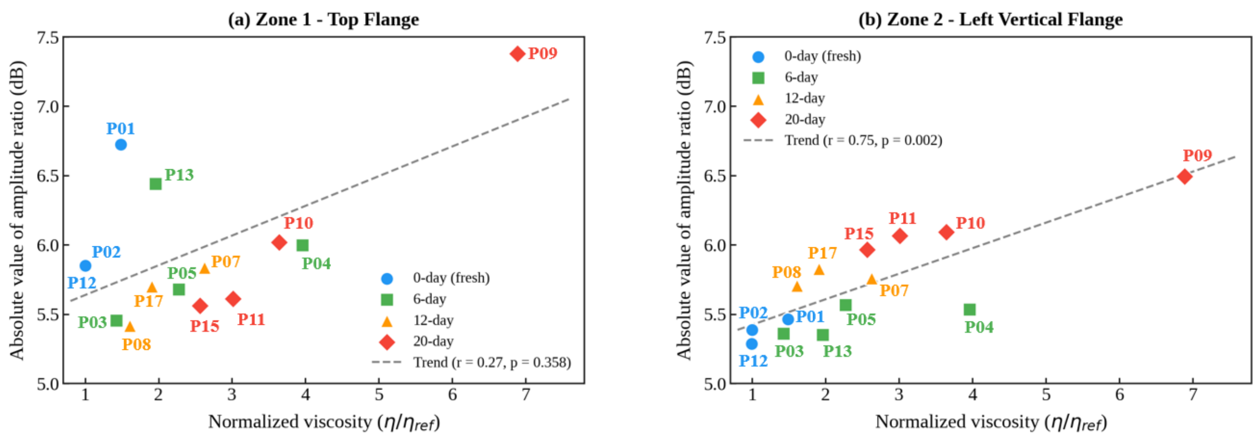

Figure 6. Absolute value of amplitude ratio as a function of normalized viscosity at consolidation onset for (a) Zone 1 - top flange and (b) Zone 2 - left vertical flange, for all 14 assessed parts.

4.3. Mechanical properties

The mechanical performance of omega-shaped parts was evaluated as a function of prepreg aging and specimen extraction location (top, vertical flanges, and foot), enabling the assessment of aging effects and potential spatial variability induced by the omega geometry (Figure 7).

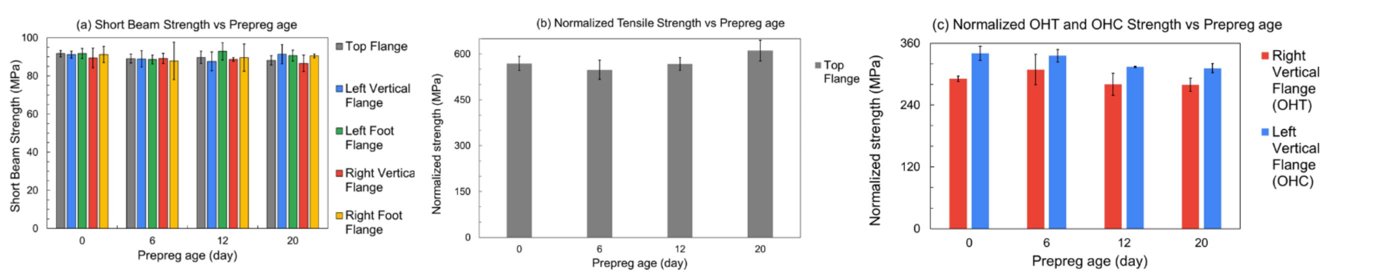

Figure 7. Mechanical properties as a function of prepreg age (a) Short beam strength, (b) Normalized unnotched tensile strength for the top flange and (c) Normalized OHT strength for the right vertical flange and OHC strength for the left vertical flange.

Short beam strength (SBS) results (Figure 7(a)) show comparable interlaminar shear performance across all 5 extraction zones for 0–20 day aging. The consistency across extraction locations indicates that the adaptive DDF process provides uniform consolidation despite the thickness transitions and geometry complexity of the omega part. This is particularly noteworthy given that SBS is expected to be sensitive to porosity, resin rich regions, and ply to ply bonding quality [9].

Normalized unnotched tensile strength results (Figure 7(b)), measured on specimens extracted from the top flange, show no significant variation with aging up to 20 days. Mean values ranged from 550 to 610 MPa across all aging stages, with a slight but non-significant increase at 20-day (+5%). This behavior is expected since UNT is a fiber dominated property and largely insensitive to resin aging. Several studies have reported that prepreg aging has minor effects on tensile-dominated properties [9–10].

A similar trend is observed for normalized open-hole tensile (OHT) and compressive (OHC) strengths (Figure 7 (c)), with limited variation as a function of prepreg aging. Strength values remain stable up to 6 days, followed by a slight decrease beyond 12 days (~5–8%). However, OHT and OHC are highly sensitive to local fiber orientation and architecture, and variations of this magnitude are commonly reported in open-hole test configurations [11]. The observed reduction is therefore not exclusively attributable to process-induced effects, resulting from a change in physical properties such as viscosity and flow index highlighted in this article, but also to the inherent variability related to the machining, preparation and testing of a limited sample size. Overall, open-hole mechanical performance remains stable across the full 0–20 day aging range.

Specimens extracted from the foot flanges systematically exhibit lower strengths than those from the vertical flanges. This can be attributed to their location (closer to the part edges) and their local forming conditions, which make them more susceptible to process-induced defects such as fiber wash-out and fiber distortion. These factors contribute to a slight reduction in mechanical performance in these regions. Note this edge boundary effect is consistent across all aging stages, confirming that it reflects geometric and process factors rather than aging-induced degradation.

The results demonstrate that the adaptive DDF strategy successfully maintains mechanical performance across the full 0–20 day aging range. SBS and UNT remain stable across all aging stages, while OHT and OHC show only minor variations within the scatter typically observed for open-hole configurations. Spatial variability between extraction locations reflects geometric and process factors inherent to the omega-shaped geometry rather than aging-induced degradation. Overall, these results confirm that model-informed parameter adaptation enables reliable manufacturing of structural composite parts using EP2750 prepreg aged up to 20 days.

5. Conclusion

This work demonstrates that model-informed adaptive DDF method effectively maintains part quality throughout the out-of-freezer aging of CYCOM® EP2750 prepreg. By adjusting preheating conditions and gap dwell duration based on model-derived viscosity and flow index, high-quality omega-shaped parts were successfully manufactured from prepreg aged up to 20 days.

Best-parameter parts from all four aging stages achieved thicknesses within ±2.4% of the reference. Ultrasonic inspection showed that top flange part quality is well maintained when appropriate parameters are applied, while vertical flange shows a slight tendency towards increased attenuation with aging that requires further cross-sectional validation. Despite the limited variations in terms of attenuation ratio, the strong viscosity - amplitude ratio correlation validates the material model indices as reliable process adaptation parameters. Mechanical testing demonstrates that the adaptive DDF method successfully preserves structural performance across the full 0–20 day aging range of EP2750 prepreg. SBS, UNT, OHT, and OHC remain within acceptable ranges across the full aging window, with minor location-dependent variability attributable to the omega geometry rather than aging. In summary, this approach supports robust processing, reduced material waste, and reliable use of aged EP2750 prepreg for more efficient and sustainable high-rate composite manufacturing.

6. References

[1] S. El Euch, Y. Jiang, K. Dupuis, B. Gourichon and F. LeBel. "Development of cure kinetics model, viscosity model and fiber bed compaction curve for CYCOM® EP2750". SAMPE Conference Proceedings, 2024.

[2] Z. Wang, Y. Li, J. Chen and L. Zhang. "A review on energy-efficient manufacturing for high-performance fiber-reinforced composites". Composites Part A: Applied Science and Manufacturing, Vol. 176, pp. 1–22, 2024.

[3] T. Obadimu, O. A. Ekuase and I. A. Adesina. "A review on the out-of-autoclave process for composite manufacturing". Polymers, Vol. 14, No. 14, Article 2926, pp. 1–29, 2022.

[4] P. Centenary, R. J. A. Clark and M. R. Wisnom. "Mitigating void growth in out-of-autoclave prepreg processing". Advanced Manufacturing: Polymer & Composites Science, Vol. 8, No. 4, pp. 185–197, 2022.

[5] C. Lopes, A. Ferreira and J. R. Correia. "Experimental investigation on the influence of out-of-autoclave process parameters on the mechanical properties of aerospace composites". Journal of Composite Materials, Vol. 58, No. 6, pp. 789–804, 2024.

[6] L. Phiri, M. Mwale and D. N. Mubanga. "Advances in lightweight composite structures and manufacturing technologies: A comprehensive review". Results in Engineering, Vol. 21, Article 101234, pp. 1–26, 2024.

[7] J. Sloan. "Solvay launches epoxy prepreg for aerostructures compression molding". CompositesWorld, February 24, 2020.

[8] C. Di Fratta, Y. Sun, P. Causse and F. Trochu. "A Dimensionless Characteristic Number for Process Selection and Mold Design in Composites Manufacturing: Part I—Theory." Journal of Composites Science, Vol. 4, No. 1, p. 11, 2020.

[9] D. Budelmann, D. Gibhardt and B. Fiedler. "A review on aging effects of thermoset prepregs". Composites Part B: Engineering, Vol. 303, Article 112611, 2025.

[10] O. A. Ekuase, N. Anjum, V. O. Eze and O. I. Okoli. "A review on out-of-autoclave composite manufacturing processes". Journal of Composite Science, Vol. 6, No. 6, Article 172, pp. 1–25, 2022

[11] K. Oine, K. Ryuzono, Y. Kawagoe, Y. Hoshikawa, K. Shirasu, Y. Takayama and T. Okabe. "Comparative study of thermosetting CF/epoxy and thermoplastic CF/PAEK composite laminates: Effects of stacking sequences on open-hole strength". Journal of Thermoplastic Composite Materials, Vol. 39, No. 1, pp. 259–291, 2026